JEE Journal of Ecological Engineering

Journal of Ecological Engineering, 2025, 26(7), 308–320
https://doi.org/10.12911/22998993/203588
ISSN 2299–8993, License CC-BY 4.0

Received: 2025.03.04
Accepted: 2025.04.30
Published: 2025.05.15

Enhancing the performance of polysulfone membrane: The role of ZIF-8 nanoparticles in biofilm control and antimicrobial activity against *Staphylococcus aureus* and *Pseudomonas aerugino*

Manar Ahmed Ehmud[1], Ghaidaa Sabry Hassoon[2], Amen Abdulrazzaq Mohammed[3], Mustafa Hussein Al-Furaiji[4*]

[1] Water, Environment, and Renewable Energy Center, Scientific Research Commission, Ministry of Higher Education and Scientific Research, Baghdad, Iraq
* Corresponding author's e-mail: alfuraiji79@gmail.com

ABSTRACT

To control biofilm in membranes through the performance enhancement of polysulfone membranes, ZIF-8 nanoparticles (NPs) were mixed into membranes. This research investigated the antimicrobial activity and biofilm dispersal capabilities of ZIF-8 nanoparticle membranes in relation to *Staphylococcus aureus* and *Pseudomonas aeruginosa.* This study used room temperature solution reaction method for synthesizing ZIF-8 NPs and characterized the materials with SEM, EDX, ZETA potential, and FTIR. Biofilm inhibition tests were conducted with results indicating that a concentration of 2.5 mg/mL ZIF-8 NPs resulted in a 99.3% inhibition rate in *Staphylococcus aureus* biofilm formation. *P. aeruginosa* biofilm formation was reduced to 96% with a higher concentration of ZIF-8 NPs at 5 mg/mL. ZIF-8 membranes (0 wt%, 0.025 wt%, 0.05 wt%, and 0.075 wt%) were fluorescently stained to visualize biofilms. The surface coverage of biofilm was (83.74%, 34.267%, 10.24%, and 43.712%) respectively, which indicated that the optimal loading of ZIF-8 NPs was (0.05 wt%). It not only improved biofilm inhibition, but also maintained the structural integrity of the membranes in this loading, whereas higher concentrations resulted in less biofilm reduction due to nanoparticle aggregation. ZIF-8 NPs integration with polysulfone increased porosity and hydrophilicity of the membrane, which in turn will reduce the bacteria's attachment to the membrane surface. There is evidence supporting the claims that ZIF-8 NPs are effective antimicrobial agents and also serve as membrane additives to tackle biofilm for water filtration and other biomedical applications.

Keywords: ZIF-8 NPs, polysulfone membrane, biofilm.

INTRODUCTION

The requirement for fresh and clean water is growing dramatically as the world's population increases (Hassoon and Al-Bayati, 2023; Kalash et al., 2020), which is quickly met by membrane separation technology. Because of its benefits, such as its great filtering effectiveness, membrane separation technology has many applications, ease of use, reduced energy consumption, affordability, and environmental friendliness (Abdul-Hussein et al., 2024; Al-Jadir et al., 2022; Al-Musawy et al., 2021). Among the most often utilized materials in membrane technology is polysulfone (PSf) (Hassan et al., 2022). It is perfect for broad usage in membrane fabrication because of its exceptional hydrolytic stability, chemical, thermal, and mechanical resistance, as well as its reasonably inexpensive cost of manufacture. Membrane fouling reduces flow, which negatively affects membrane quality, changing selectivity, raising operating costs, and reducing membrane longevity (Diwan et al., 2023). Therefore, increasing the surface hydrophilicity of membranes is a practical method of preventing fouling of membranes and enhancing the flux of water (Kadhom et al., 2021; Susanti et al., 2013; Xiong et al., 2024). The attachment and development of microbial cells on the membrane surface and holes is known as membrane biofouling. Membrane biofouling lowers membrane

efficiency, leading to financial losses and technological difficulties (Cui et al., 2021; Mahdi et al., 2022). Since pathogenic bacterial biofilms are challenging to remove because of their resilience to environmental risks, they can cause persistent infections, which is why they are now acknowledged as a significant and expensive issue for human health (Del Pozo, 2018), While the contact-type antibiofouling effects show promise in reducing bacterial surface adhesion, they are only effective against the microorganisms that come into contact with the surface, and there is a chance that the contents of their cells could leak into the treated water. Changes to the membrane interface that combine a decline in bacterial adherence with the formation of biofilms in a single phase were described by (Guo *et al.,* 2022).

Both Gram-positive and Gram-negative bacteria, including Pseudomonas and Staphylococcus species, are capable of forming biofilms. After a few free-moving bacteria come into contact with an appropriate surface, they build communication roots to acquire nutrition sources, and produce a slimy substance called extracellular polymeric substance, and biofilm formation begins (Abebe, 2020; Berne et al., 2015).

According to Vodyashkin *et al*. (2023), metal-organic frameworks (MOF) have been widely used in antimicrobial uses (Vodyashkin *et al.,* 2023). With a three-dimensional dodecahedral structure, Nanoparticles of zeolitic imidazolate frameworks -8 (ZIF-8 NPs) belong to the family of MOFs and can be produced using zinc ions and 2-methylimidazole. ZIF-8 NPs have been found to possess a variety of uses, such as adsorption (Lv et al., 2022), electrochemical sensor (Chakraborty et al., 2022), antibacterial agent, and nano-drug delivery system (Xie et al., 2022). Numerous investigations have demonstrated the potential of some nanoparticles, such as MOFs, which help spread out already-existing biofilms or stop new ones from forming (Arenas-Vivo et al., 2019; Gao et al., 2016; Mohamed et al., 2019). Long-term sterile conditions are not established when these waters are treated or disinfected for commercial usage. Therefore, membrane biofouling will result from the remaining bacteria multiplying if there is a minimal amount of nutrients available. The distinct properties of ZIF-8 NPs give PSf membranes supplemented with them notable anti-biofilm capabilities. The substantial porosity, pore size adjustability, and chemical activity of these metal-organic frameworks make them ideal for enhancing the efficiency of separating membranes biofouling (Aljumaily *et al.,* 2020; Chen et al., 2020). The objective of this research was to synthesize and describe ZIF-8 NPs as well as investigate their incorporation into PSf membranes to enhance their structural, hydrophilic, and antimicrobial properties in order to mitigate membrane biofilm.

MATERIALS AND METHODS

The preparation of ZIF-8 NPs

The solution reaction approach at room temperature was used to create ZIF-8 NPs. Firstly, 0.147 g of zinc nitrate was measured and placed in 10 mL of methanol (solution B), after weighing 0.325 g of 2-methylimidazole and dissolving it in 10 mL of methanol (solution A). ZIF-8 NPs were found in the reaction product after solution A was gradually added in 1 minute to solution B and agitated at 500 rpm for one hour at 25 °C. Following a 10-minute centrifugation with a rotational speed of 10.000 rpm, the precipitation was dissolved with methanol for a 2-minute ultrasonic treatment until it was fully dissolved.

The centrifugation and ultrasonic dissolution steps presented above were repeated twice. The methanol solution of ZIF-8 NPs was the final result of the third methanol dissolution.

ZIF-8 NPs characterization

The morphology of ZIF-8 NPs was examined utilizing a Field Emission scanning electron microscope (FE-SEM), and Both qualitative and quantitative elements were examined using Energy Dispersive X-Ray Analysis (EDX) (TESCAN MIRA3 FRENCH). The Zeta Plus Analyzer (Brookhaven, USA) was used to measure the ZIF-8 NPs diameters and the zeta potentials of each nanoparticle in water. Powder X-ray diffraction (XRD) patterns were recorded using an X-ray diffractometer (XRD 6000/SHIMADZU, Japan). FTIR spectra were collected on an FTIR spectrometer (Thermo Scientific Nicolet iS20 (USA)).

Preparation of PSf membranes

PSf membranes used in this investigation were produced using the phase inversion technique. To make the casting solution, the appropriate amount of PSF was first dissolved in a 14%

weight ratio of DMF (N, N-Dimethylformamide) solvent. The resulting mixture was left to air out at room temperature overnight after being stirred for six hours at 60 °C. With the exception of adding the appropriate quantity of nanoparticle material (0 wt%, 0.025 wt%, 0.05 wt%, and 0.075 wt%) to the casting solution before the phase inversion method, the same process was used to create the PSf-ZIF-8 membranes. The casting polymeric liquid was then poured onto a sterilized glass plate using a casting Gardner knife (also known as a film casting doctor blade), and it was cast at a thickness of 180 µm. When the glass surface containing the polymeric solution was immediately submerged in a room-temperature water bath, the flat sheet PSf membrane detached from the plate in a matter of seconds.

Characterization of PSf membranes

According to Finland's theta light (TL100 and TL101), the contact angle (CA) measures the hydrophilic qualities of the membrane. Using CA measurement, the angle between each of the membrane surfaces and the droplet generated by water was determined. At various points on the membrane sample, ten average readings were obtained, and the average was noted. The topography and microscopic examination of the membrane were investigated using FE-SEM. The membrane porosity was measured by the amount of water that was retained in the membrane after drying and comparing it to the original weight of the membrane.

Bacterial cultivation

Staphylococcus aureus and *Pseudomonas aeruginosa* was isolated and characterized by biochemical tests and VITEK® 2 Compact (bioMérieux, French). Isolates were cultured on mannitol salt agar medium and Cetrimide Agar, respectively. Individual colonies of bacteria were cultivated around 37 °C (200 rpm) after being injected in brain-heart infusion media.

Measuring the minimum inhibitory concentration (MIC)

Multiple sterile centrifuge tubes were constructed to achieve concentrations of (0.15, 0.30, 0.60, 1.25, 2.50, 5) mg mL−1 of a ZIF-8 NPs (diluted by deionized water) using the multiplicative dilution method in order to calculate MIC and sub-MIC (Turlej-Rogacka *et al.,* 2018). The centrifuge tubes holding 100 µL of ZIF-8 NPs from each concentration were filled with 100µL of bacterial culture at 1×10^7 CFU/mL. For one hour, the mixes were incubated at 37 °C. On nutrient agar, 100 µL of mixtures were spread out and kept overnight at 37 °C.

Microtiter examination for biofilm control by ZIF-8 NPs

After re-suspending bacteria with 10^7 a CFU/mL using the MIC and sub-MIC of ZIF-8 NPs solution for both bacteria, 200 µL of the bacterial culture was placed into a 96-well plate. Following 24 hours of continuous cultivation at 37 °C, Phosphate-Buffered Saline (PBS) was used three times to wash out the biofilm, and then 150 µL of 0.1% crystal violet was added, dyed for 20 minutes and then rinsed three times with PBS. Following natural drying, each hole received 200 µL of a 33% acetic acid liquid, and it was away for three minutes. The absorbance value at 580 nm was then measured using an enzyme-linked immunosorbent assay, with three replicates for each group.

Biofilm development on PSf membranes

Two different bacteria were grown together in an 18-hold nutrient broth. To achieve the required concentrations (0.001 OD), the concentration of the bacterial culture was set at 2.5×10^8 (CFU)/ml. Sterilized 100 mL tubes were filled with bacterial cultures after being vortexed (the total volume was maintained at 50 mL per tube). After being sterilized with 70% ethanol, PSf membranes containing ZIF-8 NPs (0 weight percent, 0.025 weight percent, 0.05 weight percent, and 0.075 weight percent) were submerged in sterile water and dried in a laminar flow hood, and then biofilm formation was induced on PSf membrane coupons by incubating bacterial cells at 37 °C and 120 rpm for 24 hours in 100 mL of growth media. Following incubation, the medium was taken out, and sterile water was used to wash the biofilms gently.

Measurement of cell biomass concentration on PSf membranes

Following a 24-hour incubation period, the membrane was scraped with sterilized tweezers onto the surface of a glass slide to scrape the biofilm from the top of the membrane and then it was

cut into appropriate pieces with scissors. The same tube was filled with small pieces of membrane and 20 milliliters of sterile water and vortexed for four minutes. After that, the extracts underwent a 15-minute, 10,000 rpm centrifugation at 4 °C in a centrifuge device. Biomass was the name given to the leftover pellet. Each tube holding the pellets received 10 milliliters of sterile water after the pellets had been rinsed with it. The pellets were then completely mixed in the sterilized water by vortexing. A spectrophotometer (SHIMADZU UV-1800 spectrophotometer, Japan) was used to quantify the OD (optical density) of the biomass collection at 600 nm (Barnes *et al.,* 2013).

Microscopic biofilm imaging

Microscopically, the capacity of the PSf membrane to spread biofilm formation was also confirmed by fluorescence microscopy (MEIJI TECHNO CO.,LTD, Japan). Following incubation, biofilm was stained with 0.1% fluorescein isothiocyanate (FITC) after being lightly washed with saline water and allowed to stand in a darkroom for fifteen minutes at ambient temperature. Sterilized distilled water was used to wash the slides in order to remove the unbound stain. A fluorescence microscope was then used to perform fluorescence microscopy on stained slides.

RESULTS AND DISCUSSION

Characterization of ZIF-8 NPs

ZIF-8 NPs was effectively created using the room-temperature solution reaction technique (Chen *et al.,* 2017). The ZIF-8 NPs produced in this investigation had a diameter of approximately 66.6 nm, according to FE-SEM (Figure 1a, b). The ZIF-8 NPs manufactured nanocomposite was validated by AFM (Figure 2a, b). Using the Zeta Potential, the size distribution and hydrodynamic

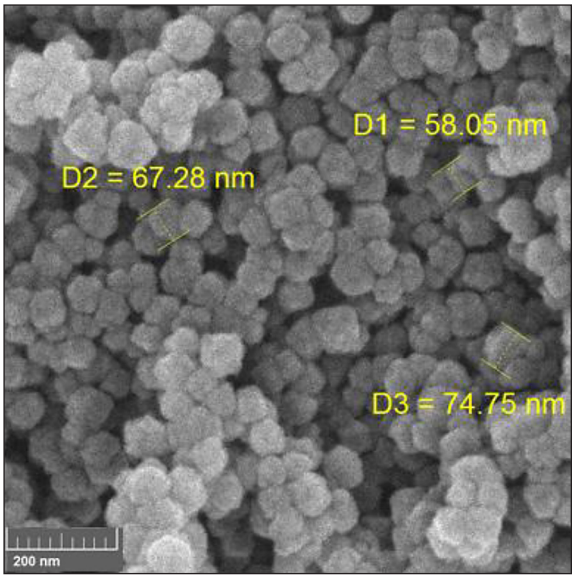

Figure 1. ZIF-8 nanoparticle scanning electron micrographs at various magnifications

size of the colloids of the nanoparticles were identified. to be 351.91 nm using dynamic light scattering (DLS) (Figure 3). The average hydrodynamic size of ZIF-8 NPs was greater than the size determined by SEM images because of their aggregation in water (Saliba *et al.,* 2018).

XRD was used to determine the crystallinity of the material (Figure 3a). The crystallographic data of the compound showed a cubic crystal system with space group number 217 (I-43m), and the peaks had a good match with the COD 4118892 database card, verifying that ZIF-8 is a characteristic of zeolitic imidazolate frameworks. The chemical formula name was $Zn_{12.00}N_{48.00}C_{75.60}H_{79.80}$, which implies a variation in the stoichiometry when compared with conventional ZIF-8. The structural data closely matches the outcomes reported by Karagiaridi *et al.,* (2012) (Karagiaridi *et al.,* 2012). According to the EDX results, the material is mostly made up of carbon and nitrogen, with trace levels of zinc (Figure 3b), which supported the XRD results.

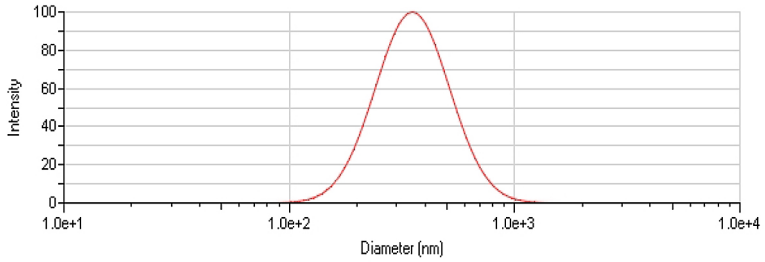

Figure 2. Dynamic light scattering (DLS) dispersion of ZIF-8 particle diameter in Zeta Potential

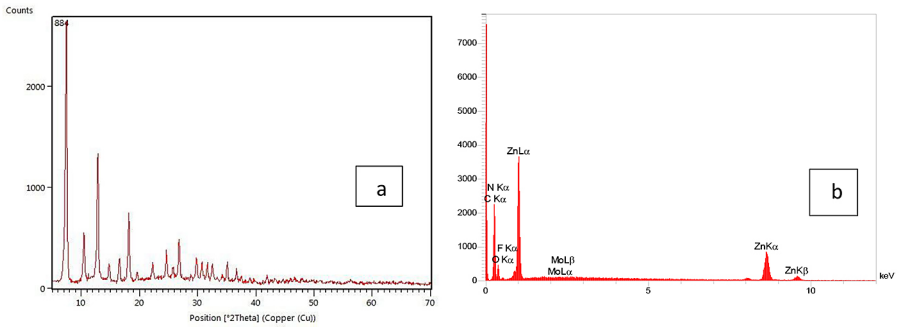

Figure 3. (a) X-ray diffraction pattern of ZIF-8; (b) an EDX plot verifying the fundamental composition of ZIF-8 nanoparticles

The effectively synthesized ZIF-8 NPs were validated via the FT-IR spectra, which also revealed information on the functional groups and chemical structure (Figure 4). The aromatic and aliphatic C–H stretches of imidazole group are attributed to the weakened bands at 3138 and 2933 cm^{-1}, respectively. Imidazole ring stretching is responsible for the complex bands between 1350 and 1500 cm^{-1}, whereas C=N stretching is responsible for the peak at 1585 cm^{-1}. The bands in the 900–1350 cm^{-1} range are associated with both in-plane and out-of-plane bending of the imidazole ring and below 850 cm^{-1} regions, respectively. Zn–N stretching is associated with a prominent band at 420 cm^{-1}. These outcomes were in line with those of Hu *et al*. (2011).

The description of membranes made of polysulfone (PSf)

Figures A and B show the surface of membranes with incorporated ZIF-8 NPs and pristine membranes, respectively. The surface of PSF membranes in Figure 5 A shows a dense PSf membrane structure and does not seem to contain any particulate structures. However, the ZIF-8 NP-loaded membrane (Figure 5 B) shows elevated levels of particulate structures and distributed small particles, which indicate that the surface is heterogeneously rough. These results imply the successful incorporation of ZIF-8 NPs into the membrane matrix. Cross-sectional SEM pictures of the polysulfone membrane taken with and without ZIF-8 NPs are displayed in Figures 5C and D, respectively. The interior structure of the membranes can be understood via cross-sectional SEM pictures. A dense, compact structure with comparatively little porosity is evident in the pristine PSf membrane (Figure 5C), which is indicative of a phase-inversion process. Nevertheless, the cross-section of the ZIF-8-modified membrane (Figure 5D) shows a more interconnected and porous structure, with a discernible rise in voids and finger-like channels. ZIF-8 NPs seem to improve phase separation during membrane formation, which encourages the creation of a more porous structure.

Any changes in the structure and the chemical interaction of the membranes with various doses of ZIF-8 NPs were studied using FTIR spectra

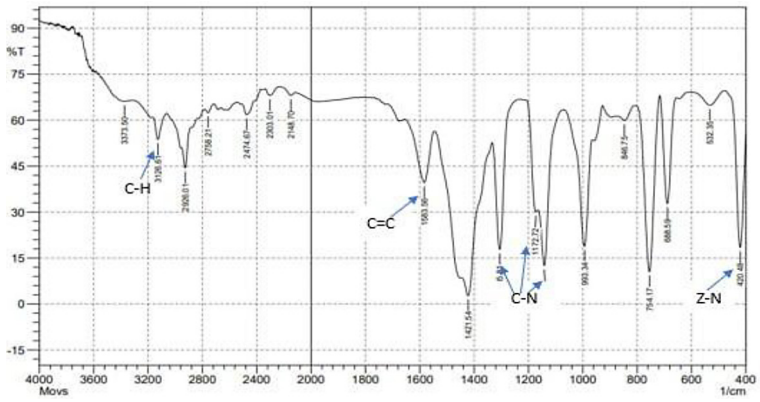

Figure 4. FT-IR spectrum of ZIF-8 NPs

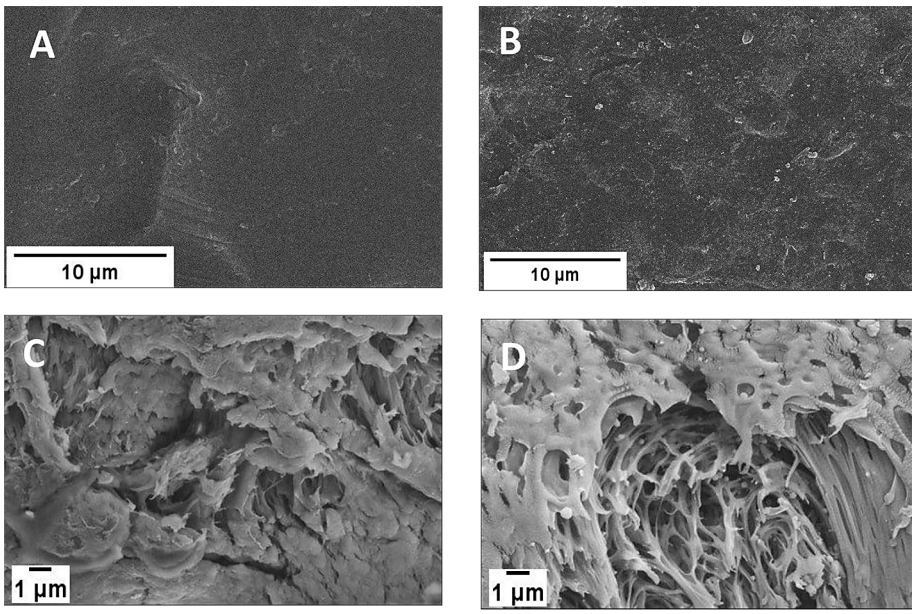

Figure 5. FE-SEM images A. Surface view of the control membrane with 0.00 wt% free of ZIF-8 type difference particles. B. PSf-ZIF-8 membrane containing 0.05 wt% ZIF-8 type difference particles. C. Cross-section of the control membrane with 0.00 wt% free of ZIF-8 type difference particles. D. Cross-section of 0.00 wt% ZIF-8 type difference particles

with ZIF-8 NP loadings of 0.0 wt%, 0.025 wt%, 0.05 wt%, and 0.075 wt%. In the case of 0.0 wt%, there is a very low weight percentage, and no sign of ZIF-8-specific peaks can be discerned. Meanwhile, various characteristic peaks of PSf membranes, such as aromatic C=C bands, S=O stretch, and C-O-C bonds, can be seen (Figure 6a). The total increase in OH vibrations on stretching, which suggests weak hydrogen bonding, shows that a 0.025 wt% membrane has a low ZIF-8 NPs concentration. There is also a change in the band at 1600–1500 cm^{-1} associated with C=N, which is a sign of ZIF-8 NPs integration (Figure 6 b). The membranes at both the 0.005 wt% and 0.075 wt% ZIF-8 NPs demonstrate a peak at the range of 960 cm^{-1}, which is linked to Zn-N expansion,

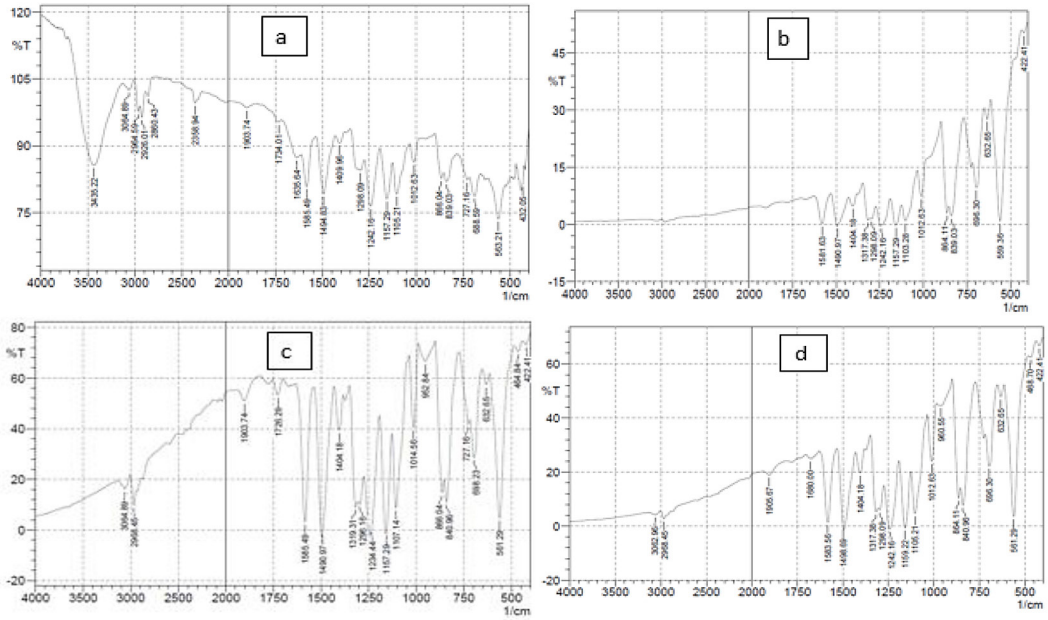

Figure 6. FT-IR spectrum of PSf membranes. a. 0.00 wt% ZIF-8 NPs (Control Membrane). b. 0.025 wt% ZIF-8 NPs membrane. c. 0.05 wt% ZIF-8 NPs membrane. d. 0.075 wt% ZIF-8 NPs membrane

which validates the successful incorporation of ZIF-8's inside the polymer matrix (Figure 6 c, d). More noticeable in the 0.075 wt% ZIF-8 NPs, a peak at 696 cm^{-1} indicates the expected Zn-O or Zn-N bonds in ZIF-8 NPs frameworks. A tentative argument supporting potential interactions between PSf matrix and ZIF-8 NPs is derived from the slight shifting of the band at 1585 cm^{-1} to 1583 cm^{-1} in the membranes ZIF-8 NP. This change can be attributed to surface interactions or hydrogen bonding (Figure 6d).

At 1680 cm^{-1}, a new peak appears in the 0.075 weight percent ZIF-8 NPs membrane that was absent from the lower concentration sample may suggest increased interaction between ZIF-8 NPs and functional groups within the polymer structure. These results lend credence to the idea that ZIF-8 NPs nanoparticles physically incorporate into the membrane and engage in chemical interactions with the polymer matrix, which may improve the transportation, mechanical strength, and chemical resistance of a membrane (Cong *et al.,* 2020; Xiong *et al.,* 2024).

The water CA was measured in order to assess the wettability of PSf membranes at varying ZIF-8 nanoparticle loadings (Figure 7). The contact angle of a pristine membrane 0.0 wt% was around 84°, indicating moderate hydrophobicity, because the hydrophobic characteristics of PSf are widely known and can lead to issues like adsorptive fouling in membranes used for microfiltration and ultrafiltration (Dmitrieva *et al.,* 2022). In the membrane 0.025 wt% ZIF-8, the contact angle decreased to about 67°, suggesting improved hydrophilicity due to the incorporation of ZIF-8. This improvement was attributable to the hydrophilic nature of ZIF-8 nanoparticles and their even dispersion, which enhances surface energy. The CA in the 0.05 wt% ZIF-8 membrane was further decreased to roughly 58°, reflecting a progressive enhancement in hydrophilicity. Tarkhani *et al.,* 2023 found that incorporating ZIF-8 into polysulfone membranes enhanced hydrophilicity, as demonstrated by the water CA dropping from 64.4° to 51.2°. This is attributed to the increased surface roughness and the presence of hydrophilic functional groups on the ZIF-8 surface (Makhetha and Moutloali, 2021). A slight rise in CA was revealed in the 0.075 wt% ZIF-8 membrane with values of almost 74°. This could result from nanoparticle aggregation at higher loadings, reducing the effective hydrophilic surface area and leading to non-uniform coverage, which reduces interfacial compatibility, leading to decreased hydrophilicity and permeability due to poor connectivity among the nanoparticles (Jonnalagedda and Kuncharam, 2023).

The incorporation of ZIF-8 nanoparticles significantly impacts the porosity of polysulfone membranes, as shown in Figure 8. Porosity is a critical parameter for membrane performance, influencing water permeability, fouling resistance, and the ability to resist biofilm formation. The pristine polysulfone membrane without ZIF-8 exhibits a porosity of 55%. This relatively low porosity reflects the compact nature of the membrane structure. At 0.025 wt% ZIF-8 loading, the porosity increases to 60%, indicating the successful integration of nanoparticles within a matrix of polymers. The presence of ZIF-8 nanoparticles. The membrane at 0.05 wt% ZIF-8 shows the highest porosity at 70%. This significant increase was attributable to the optimal dispersion of ZIF-8, which creates interconnected voids within the

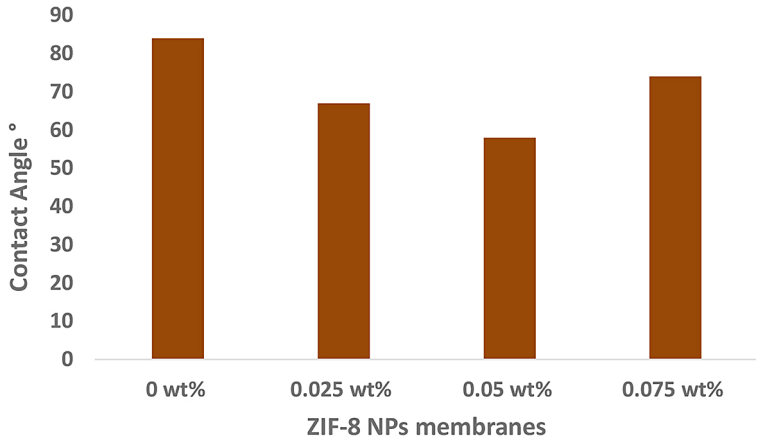

Figure 7. Contact angle measurements for PSf membranes for different ZIF-8 NPs membranes

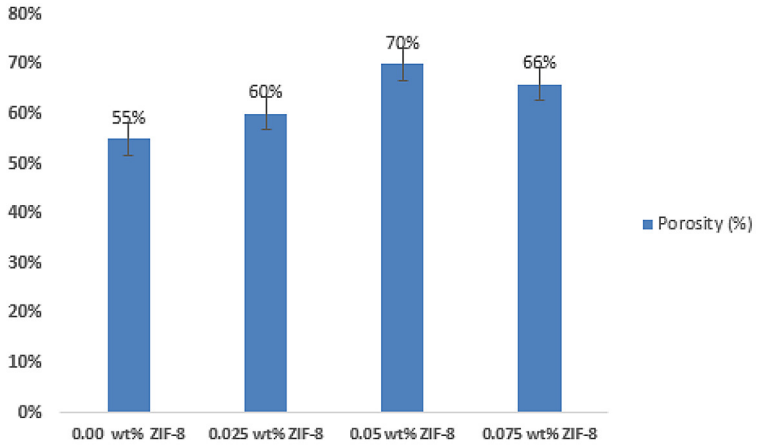

Figure 8. Porosity of polysulfone membranes with different ZIF-8 nanoparticle loadings

polymer matrix. With 0.075 wt% ZIF-8, the porosity decreases slightly to 66%. This reduction is likely due to nanoparticle aggregation, as observed in the SEM images. Excessive ZIF-8 loading can lead to uneven dispersion, causing particle clusters to occupy pore spaces, reducing the effective porosity (Zhan *et al.,* 2023).

ZIF-8 forms a continuous layer on the surface of the membrane, which raises roughness and alters the morphology of the membrane. This structural change contributes to enhanced porosity (Li *et al.,* 2017; Wang *et al.,* 2020). In addition, it could increase the rough texture of the surface and hydrophilicity of the membrane, which can improve water flux and reduce bacterial adhesion, thereby enhancing antibacterial properties (Aljumaily *et al.,* 2020). These enhancements lead to improved antifouling properties and water permeability, making these membranes highly effective for applications in water treatment and antimicrobial applications (Wang *et al.,* 2016).

Antibacterial activity against bacteria and MIC of ZIF-8 NPs

ZIF-8 NPs reduced both the Gve^- bacteria *Pseudomonas aeruginosa* and the Gve^+ bacteria *Staphylococcus aureus* by multiplicative dilution method. The amounts of (0.15, 0.30, 0.60, 1.25, 2.50, 5) mg/mL at which the substance could suppress bacterial growth varied, even while it was capable of killing the tested bacteria at increasing quantities. *S. aureus* has a minimum inhibitory concentration (MIC) of 2.5 mg/mL with a sub-MIC of 1.25 mg/mL, whereas *P. aeruginosa* has a MIC of 5 mg/mL with a sub-MIC of 2.5 mg/mL (Figure 9). The result shows that ZIF-8 NPs was more effective elimination on the Gve+ bacteria

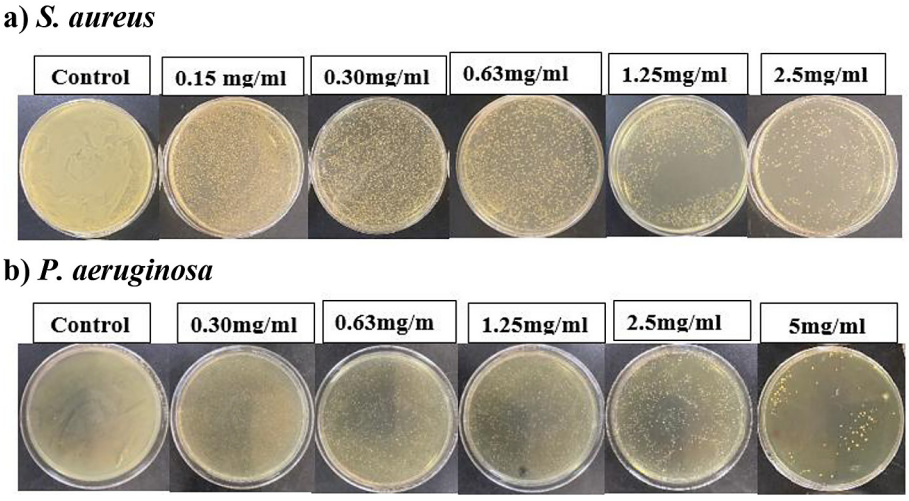

Figure 9. Pictures of bacterial colonies following treatment with varying ZIF-8 concentrations for two distinct species. a. *P. aeruginosa* b. *S. aureus*

Staphylococcus aureus than Gve⁻ bacteria *Pseudomonas aeruginosa*.

In general, ZIF-8 NPs can infiltrate cells and harm them, and because Gram-positive bacteria lack an outer cell membrane, they are more susceptible to this invasion (Chowdhuri *et al.,* 2017; Singbumrung *et al.,* 2018). According to earlier research, ZIF-8 NPs have a bactericidal effect because zinc ions can pass through ion channels across bacterial membranes, using additional energy and upsetting the bacteria (Ma *et al.,* 2009). Certain ZIF-8 NPs were more efficient against Gve⁺ bacteria than Gve⁻ ones, based on earlier research (Chowdhuri *et al.,* 2017; Shen *et al.,* 2020). According to the authors' hypothesis, ZIF-8 NPs may be prevented from diffusing into Gram-negative bacteria cells by their outer protective membrane (Singbumrung *et al.,* 2018).

ZIF-8 inhibits bacteria biofilm formation

The conducted investigation demonstrated that *Pseudomonas aeruginosa* and *Staphylococcus aureus* could develop a robust bacterial biofilm at 24 hours, with ODCs of 0.33 and 1.46, respectively, based on control optical density (OD). The ZIF-8 NPs treatment group's biofilm for both bacteria was considerably lower than that of the control one, according to the Crystal Violet stain solution outcomes. Following the dissolution of crystal violet, the biofilm development was assessed. OD is 0.003 at a dosage of 2.5 mg/mL of ZIF-8 NPs, indicating a 99.3% inhibition rate of *Staphylococcus aureus* development of biofilm. With a dose of 2.5 mg/mL and an OD of 0.1, ZIF-8 NPs may inhibit *P. aeruginosa* biofilm development by 70%, while with a higher dose of 5 mg/mL and an OD of 0.01 it can inhibit *P. aeruginosa* biofilm formation by 96% (Figure 10 a, b). According to previous studies, ZIF-8 NPs can inhibit the formation and disperse established biofilms by reducing the expression of adhesion-related proteins and inhibiting pathways like arginine biosynthesis, which are crucial for biofilm stability (Tian *et al.,* 2024). Additionally, ZIF-8 nanoparticles may destroy biofilms by breaking down the extracellular DNA (eDNA) in the biofilm structure (Gokhale *et al.,* 2024).

ZIF-8 NPs reinforced PSf membranes hinder bacteria biofilm

The purpose of this study was to identify how ZIF-8 NPs would enhance the polysulfone membranes against the cell biomass of hybrid bacteria. The ZIF-8 NPs membranes (0 wt%, 0.025 wt%, 0.05 wt%, and 0.075 wt%) were investigated according to Siddiqui *et al*. (2015), which measured biomass reduction in membrane coupons by optical density (OD) of a spectrophotometer (Figure 11). After being separated from membranes, the biomass of biofilms was assessed (OD) at 600 nm, and the inhibition rate was calculated. The 0 wt% membranes exhibited the maximum biofilm development when ZIF-8 NPs were not present. It was observed that membranes at 0.025 wt% of ZIF-8 NPs were lowered by 38% of biomass on the membrane surface, but membranes at 0.075 wt% were slightly lowered by 15.5% of biomass, and membranes at 0.05 wt% demonstrated the highest inhibition rate of biofilm with rate of 63%. Biofilm elimination was further examined under a fluorescence microscope as illustrated in (Figure 12). The ZIF-8 NPs membranes were dyed, placed on glass slides so that the biofilm faced up, and viewed at 400× magnification.

Fluorescence microscopic images were processed with ImageJ software (Garcez *et al.,* 2020). The biomass surface covering at 0.0 wt% was found to be 83.7%, while the biomass at 0.05

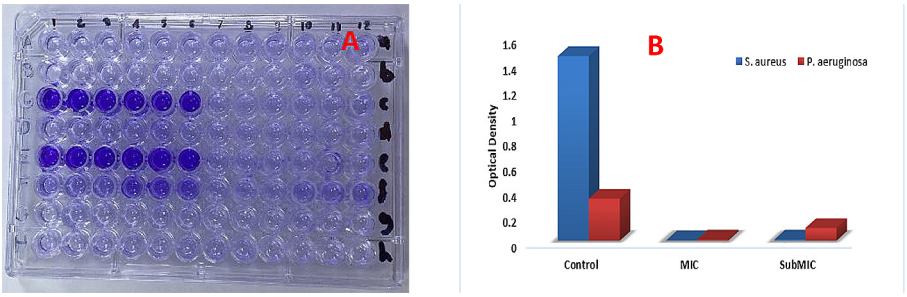

Figure 10. A. Tissue culture plate for detecting the production of biofilms by *P. aeruginosa* and *S. aureus* bacteria. B. The image shows Mic, Sub Mic of two different bacteria by measuring the optical density of the tissue culture plate at a wavelength of 580 nm

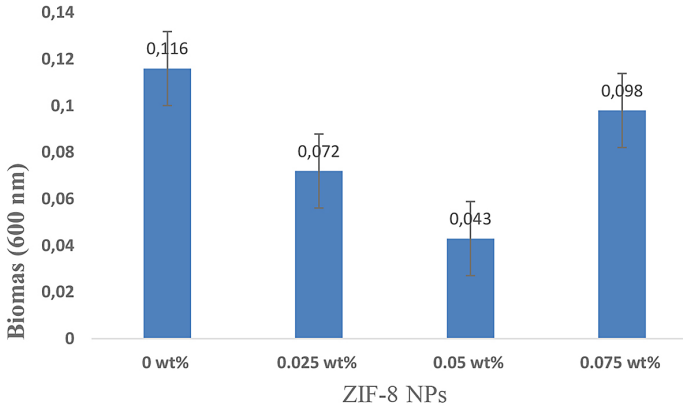

Figure 11. The impact of different ZIF-8 NPs on PSf membranes in the 24 hour biofilm biomass dispersal

wt% membrane was 10.24% (Table 1). The 0.0 wt% membrane, as illustrated in the image in Figure 12a, exhibits a high biofilm density, suggesting that active bacterial colonies are producing a strong biofilm. The biofilm coverage surface was (34.26%, 43.71%) at the (0.025 wt%, 0.075 wt%) membranes as shown in (Figure 12 b,d); they were shown to be substantially less than control in the biomass surface coverage (Table 1).

At 0.05 wt% ZIF-8 NPs membrane, the inhibition rate reaches its maximum, indicating an optimal concentration of ZIF-8 NPs. The nanoparticles are likely well-dispersed at this concentration, allowing for uniform antimicrobial activity across the membrane surface. Improved hydrophilicity (as shown by contact angle data) also enhances anti-biofouling performance by reducing bacterial adhesion. This concentration strikes a balance between nanoparticle availability, surface uniformity, and hydrophilicity. Increased hydrophilicity prevents the colonization of microorganisms. It might be argued that if the membrane surface is extremely hydrophilic, a layer of water molecules will stick to it, preventing bacteria from adhering and secreting their extracellular polymeric materials. Eventually, this would lead to an inadequate level of biofilm production, which is necessary for the maturation of biofouling mechanisms (Flemming, 2002). The hydrophilic nature of ZIF-8 NPs nanoparticles contributes to improved water flux and fouling resistance by creating a more water-attractive surface, which discourages foulant deposition (Akbari and Peyravi, 2020; Zhang *et al.,* 2021). The improved porosity enhances both water flux and fouling resistance, as the larger pore structure

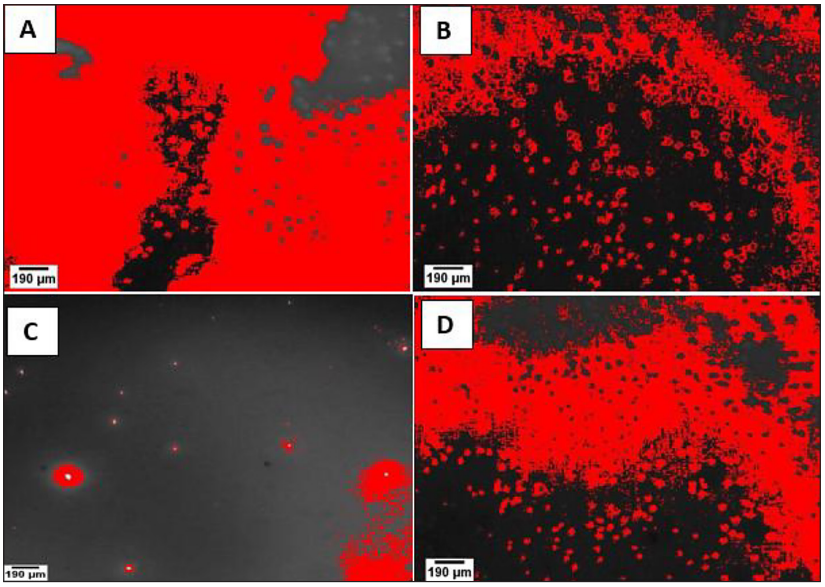

Figure 12. Fluorescence microscopic visualization of PSf membranes with different weight percentage of ZIF-8 NPs showing biofilm dispersion on them. (a) 0.00 wt%, (b) 0.025wt%, (c) 0.050 wt%, (d) 0.075 wt%

Table 1. The surface coverage of biofilm calculated by ImageJ on PSf membranes with different wt% of ZIF-8NPs

PSF membranes (wt%)	Surface coverage of biofilm (%)
0	83.7
0.025	34.3
0.05	10.2
0.075	43.7

reduces the accumulation of bacterial cells and other foulants. The structural stability and porosity of ZIF-8 NPs provide additional pathways for water molecules, enhancing overall membrane performance (Makhetha and Moutloali, 2021).

On the other hand, casting membrane 0.075 wt% using high loading ZIF-8 NPs can cause the ZIF-8 NPs to aggregate, which would leave the membrane matrix with an irregular and non-homogenized distribution (Kim and Van der Bruggen, 2010). As it was previously mentioned, ZIF-8 NPs operate to improve hydrophilicity. PSf membranes combined with ZIF-8 NPs membranes would no longer have the anti-adhesive qualities since the surface areas devoid of ZIF-8 NPs would not have these improved characteristics. In addition, increasing the percentage of ZIF-8NPs causes a rise in the aggregation rate, as shown by the SEM images, and this aggregation leads to a decrease in mechanical strength and may obstruct the membrane pores, which affects the permeability (Wan *et al.,* 2023).

CONCLUSIONS

This study successfully synthesized and characterized ZIF-8 NPs, demonstrating their strong antibacterial and anti-biofilm properties, particularly against *S. aureus* and *P. aeruginosa*. The incorporation of ZIF-8 NPs into polysulfone membranes enhanced their biofilm resistance and hydrophilicity. Optimal ZIF-8 loading (0.05 wt%) achieved a balance between biofilm inhibition and structural integrity, while higher concentrations (0.075 wt%) showed slight biofilm reduction but potential nanoparticle aggregation. These results underscore the promise of ZIF-8 NPs as effective antimicrobial agents and membrane additives for addressing biofouling in water filtration systems and other biomedical applications. Future studies should focus on scaling production and testing performance under real-world conditions.

REFERENCES

1. Abdul-Hussein, S. T., Al-Furaiji, M. H., Meskher, H., Ghernaout, D., Fal, M., ALotaibi, A. M. & Alsalhy, Q. F. (2024). Prospects of forward osmosis-based membranes for seawater mining: Economic analysis, limitations and opportunities. *Desalination*, *579*, 117477. https://doi.org/10.1016/j.desal.2024.117477
2. Abebe, G. M. (2020). The role of bacterial biofilm in antibiotic resistance and food contamination. *International Journal of Microbiology*, 1–10. https://doi.org/10.1155/2020/1705814
3. Akbari, S. & Peyravi, M. (2020). Improving water flux and salt rejection by a tradeoff between hydrophilicity and hydrophobicity of sublayer in TFC FO membrane. *Chemical Engineering Research and Design*, *162*, 94–106. https://doi.org/10.1016/j.cherd.2020.08.001
4. Al-Jadir, T., Alardhi, S. M., Alheety, M. A., Najim, A. A., Salih, I. K., Al-Furaiji, M. & Alsalhy, Q. F. (2022). Fabrication and characterization of polyphenylsulfone/titanium oxide nanocomposite membranes for oily wastewater treatment. *Journal of Ecological Engineering*, *23*(12), 1–13. https://doi.org/10.12911/22998993/154770
5. Aljumaily, M. M., Alsaadi, M. A., Binti Hashim, N. A., Mjalli, F. S., Alsalhy, Q. F., Khan, A. L. & Al-Harrasi, A. (2020). Superhydrophobic nanocarbon-based membrane with antibacterial characteristics. *Biotechnology Progress*, *36*(3). https://doi.org/10.1002/btpr.2963
6. Al-Musawy, W. K., Al-Furaiji, M. H. & Alsalhy, Q. F. (2021). Synthesis and characterization of PVC-TFC hollow fibers for forward osmosis application. *Journal of Applied Polymer Science*, *138*(35), 1–15. https://doi.org/10.1002/app.50871
7. Arenas-Vivo, A., Amariei, G., Aguado, S., Rosal, R. & Horcajada, P. (2019). An Ag-loaded photoactive nano-metal organic framework as a promising biofilm treatment. *Acta Biomaterialia*, *97*, 490–500. https://doi.org/10.1016/j.actbio.2019.08.011
8. Berne, C., Ducret, A., Hardy, G. G. & Brun, Y. V. (2015). Adhesins Involved in Attachment to Abiotic Surfaces by Gram-Negative Bacteria. *Microbiology Spectrum*, *3*(4). https://doi.org/10.1128/microbiolspec.MB-0018-2015
9. Chakraborty, T., Das, M., Lin, C.-Y., Su, Y., Yuan, B. & Kao, C.-H. (2022). ZIF-8 nanoparticles based electrochemical sensor for non-enzymatic creatinine detection. *Membranes*, *12*(2), 159. https://doi.org/10.3390/membranes12020159
10. Chen, F., Dong, S., Wang, Z., Xu, J., Xu, R. & Wang, J. (2020). Preparation of mixed matrix composite membrane for hydrogen purification by incorporating ZIF-8 nanoparticles modified with tannic acid. *International Journal of*

Hydrogen Energy, *45*(12), 7444–7454. https://doi.org/10.1016/j.ijhydene.2019.04.050

11. Chen, J., Zhang, X., Huang, C., Cai, H., Hu, S., Wan, Q., Pei, X. & Wang, J. (2017). Osteogenic activity and antibacterial effect of porous titanium modified with metal-organic framework films. *Journal of Biomedical Materials Research Part A*, *105*(3), 834–846. https://doi.org/10.1002/jbm.a.35960
12. Chowdhuri, A. R., Das, B., Kumar, A., Tripathy, S., Roy, S. & Sahu, S. K. (2017). One-pot synthesis of multifunctional nanoscale metal-organic frameworks as an effective antibacterial agent against multidrug-resistant *Staphylococcus aureus*. *Nanotechnology*, *28*(9), 095102. https://doi.org/10.1088/1361-6528/aa57af
13. Cong, S., Shen, Q., Shan, M., Wang, J., Liu, J. & Zhang, Y. (2020). Enhanced permeability in mixed matrix membranes for CO2 capture through the structural regulation of the amino-functionalized Co/ZIF-8 heterometallic nanoparticles. *Chemical Engineering Journal*, *383*, 123137. https://doi.org/10.1016/j.cej.2019.123137
14. Cui, Y., Gao, H., Yu, R., Gao, L. & Zhan, M. (2021). Biological-based control strategies for MBR membrane biofouling: a review. *Water Science and Technology*, *83*(11), 2597–2614. https://doi.org/10.2166/wst.2021.168
15. Del Pozo, J. L. (2018). Biofilm-related disease. *Expert Review of Anti-Infective Therapy*, *16*(1), 51–65. https://doi.org/10.1080/14787210.2018.1417036
16. Diwan, T., Abudi, Z. N., Al-Furaiji, M. H. & Nijmeijer, A. (2023). A competitive study using electrospinning and phase inversion to prepare polymeric membranes for oil removal. *Membranes*, *13*(5). https://doi.org/10.3390/membranes13050474
17. Flemming, H.-C. (2002). Biofouling in water systems – cases, causes and countermeasures. *Applied Microbiology and Biotechnology*, *59*(6), 629–640. https://doi.org/10.1007/s00253-002-1066-9
18. Gao, L., Liu, Y., Kim, D., Li, Y., Hwang, G., Naha, P. C., Cormode, D. P. & Koo, H. (2016). Nanocatalysts promote Streptococcus mutans biofilm matrix degradation and enhance bacterial killing to suppress dental caries in vivo. *Biomaterials*, *101*, 272–284. https://doi.org/10.1016/j.biomaterials.2016.05.051
19. Garcez, A. S., Barros, L. C., Fernandes, M. R. U., Fujii, D. N., Suzuki, S. S. & Nepomuceno, R. (2020). Fluorescence image and microbiological analysis of biofilm retained around healthy and inflamed orthodontic miniscrews. *Photodiagnosis and Photodynamic Therapy*, *30*, 101707. https://doi.org/10.1016/j.pdpdt.2020.101707
20. Gokhale, K. M., Patravale, V., Pingale, R., Pandey, P. & Vavilala, S. L. (2024). Se-functionalized ZIF-8 nanoparticles: synthesis, characterization and disruption of biofilms and quorum sensing in Serratia marcescens. *Biomedical Materials*, *19*(5), 055020. https://doi.org/10.1088/1748-605X/ad6549
21. Guo, Y., Liu, C., Liu, H., Zhang, J., Li, H. & Zhang, C. (2022). Contemporary antibiofouling modifications of reverse osmosis membranes: State-of-the-art insights on mechanisms and strategies. *Chemical Engineering Journal*, *429*, 132400. https://doi.org/10.1016/j.cej.2021.132400
22. Hassan, M. M., Abudi, Z. N., Al-Furaiji, M. H., Info, A., Mohammed, H. A., Sachit, D. E. & Al-Furaiji, M. H. (2022). Studying the performance of various polymeric ultrafiltration membranes in dye removal. *Desalination and Water Treatment*, *280*, 139–156. https://doi.org/10.5004/dwt.2022.29076
23. Hassoon, G. S. & Al-Bayati, Y. K. (2023). Synthesis, Characterization and Application of Calcium Ion-Imprinted Polymeric Solid-Phase Extraction and Pre-Concentration in Aqueous Solutions by Packed-Bed Columns. *Iraqi Journal of Science*, 5462–5475. https://doi.org/10.24996/ijs.2023.64.11.1
24. Hu, Y., Kazemian, H., Rohani, S., Huang, Y. & Song, Y. (2011). In situ high pressure study of ZIF-8 by FTIR spectroscopy. *Chemical Communications*, *47*(47), 12694. https://doi.org/10.1039/c1cc15525c
25. Jonnalagedda, A. & Kuncharam, B. V. R. (2023). Investigation of ZIF-8, amine-modified ZIF-8 and polysulfone based mixed matrix membranes for CO_2/CH_4 separation. *Journal of Applied Polymer Science*, *140*(45). https://doi.org/10.1002/app.54650
26. Kadhom, A. M., Al-Furaiji, M. H. & Abudi, Z. N. (2021). Evaluation of thin film composite forward osmosis membranes: effect of polyamide preparation conditions. *Drinking Water Engineering and Science*, *14*(1), 45–52. https://doi.org/10.5194/dwes-14-45-2021
27. Kalash, K. R., Al-Furaiji, M. H., Waisi, B. I. & Ali, R. A. (2020). Evaluation of adsorption performance of phenol using non-calcined Mobil composition of matter no. 41 particles. *Desalination and Water Treatment*, *198*, 232–240. https://doi.org/10.5004/dwt.2020.26018
28. Karagiaridi, O., Lalonde, M. B., Bury, W., Sarjeant, A. A., Farha, O. K. & Hupp, J. T. (2012). Opening ZIF-8: A Catalytically Active Zeolitic Imidazolate Framework of Sodalite Topology with Unsubstituted Linkers. *Journal of the American Chemical Society*, *134*(45), 18790–18796. https://doi.org/10.1021/ja308786r
29. Li, Y., Wee, L. H., Martens, J. A. & Vankelecom, I. F. J. (2017). Interfacial synthesis of ZIF-8 membranes with improved nanofiltration performance. *Journal of Membrane Science*, *523*, 561–566. https://doi.org/10.1016/j.memsci.2016.09.065
30. Lv, X., Zhang, Y., Wang, X., Hu, L. & Shi, C. (2022). Multilayer graphene oxide supported ZIF-8 for efficient removal of copper ions. *Nanomaterials*, *12*(18), 3162. https://doi.org/10.3390/nano12183162

31. Ma, Z., Jacobsen, F. E. & Giedroc, D. P. (2009). Coordination chemistry of bacterial metal transport and sensing. *Chemical Reviews*, *109*(10), 4644–4681. https://doi.org/10.1021/cr900077w
32. Makhetha, T. A. & Moutloali, R. M. (2021). Incorporation of a novel Ag–Cu@ZIF-8@GO nanocomposite into polyethersulfone membrane for fouling and bacterial resistance. *Journal of Membrane Science*, *618*, 118733. https://doi.org/10.1016/j.memsci.2020.118733
33. Mohamed, N., Timofeyeva, Y., Jamrozy, D., Rojas, E., Hao, L., Silmon de Monerri, N. C., Hawkins, J., Singh, G., Cai, B., Liberator, P., Sebastian, S., Donald, R. G. K., Scully, I. L., Jones, C. H., Creech, C. B., Thomsen, I., Parkhill, J., Peacock, S. J., Jansen, K. U., … Anderson, A. S. (2019). Molecular epidemiology and expression of capsular polysaccharides in Staphylococcus aureus clinical isolates in the United States. *PLOS ONE*, *14*(1), e0208356. https://doi.org/10.1371/journal.pone.0208356
34. Saliba, D., Ammar, M., Rammal, M., Al-Ghoul, M. & Hmadeh, M. (2018). Crystal Growth of ZIF-8, ZIF-67, and Their Mixed-Metal Derivatives. *Journal of the American Chemical Society*, *140*(5), 1812–1823. https://doi.org/10.1021/jacs.7b11589
35. Shen, M., Forghani, F., Kong, X., Liu, D., Ye, X., Chen, S. & Ding, T. (2020). Antibacterial applications of metal–organic frameworks and their composites. *Comprehensive Reviews in Food Science and Food Safety*, *19*(4), 1397–1419. https://doi.org/10.1111/1541-4337.12515
36. Singbumrung, K., Motina, K., Pisitsak, P., Chitichotpanya, P., Wongkasemjit, S. & Inprasit, T. (2018). Preparation of Cu-BTC/PVA Fibers with Antibacterial Applications. *Fibers and Polymers*, *19*(7), 1373–1378. https://doi.org/10.1007/s12221-018-8072-8
37. Susanti, R. F., Han, Y. S., Kim, J., Lee, Y. H. & Carbonell, R. G. (2013). A new strategy for ultralow biofouling membranes: Uniform and ultrathin hydrophilic coatings using liquid carbon dioxide. *Journal of Membrane Science*, *440*, 88–97. https://doi.org/10.1016/j.memsci.2013.03.068
38. Tian, X., Liu, B., Wu, H., Cai, R., Yang, Y., Zhou, C., Zhao, Z., Bai, Q., Wang, Y. & Liu, T. (2024). Zinc imidazole Framework-8 nanoparticles disperse mrsa biofilm by inhibiting arginine biosynthesis and down-regulating adhesion-related proteins. *Advanced Materials Interfaces*, *11*(14). https://doi.org/10.1002/admi.202300957
39. Turlej-Rogacka, A., Xavier, B. B., Janssens, L., Lammens, C., Zarkotou, O., Pournaras, S., Goossens, H. & Malhotra-Kumar, S. (2018). Evaluation of colistin stability in agar and comparison of four methods for MIC testing of colistin. *European Journal of Clinical Microbiology & Infectious Diseases*, *37*(2), 345–353. https://doi.org/10.1007/s10096-017-3140-3
40. Vodyashkin, A. A., Sergorodceva, A. V., Kezimana, P. & Stanishevskiy, Y. M. (2023). Metal-organic framework (MOF)—A universal material for biomedicine. *International Journal of Molecular Sciences*, *24*(9), 7819. https://doi.org/10.3390/ijms24097819
41. Wan, Z.-H., Guan, J., Zhang, C.-M., Fei, W.-Q., Wang, L., Wang, S.-G. & Sun, X.-F. (2023). Establishing a high-performance anti-fouling PEI-ZIF-PAA membrane with improved Lewis acid-base interactions and hydrophilicity. *Chemosphere*, *314*, 137545. https://doi.org/10.1016/j.chemosphere.2022.137545
42. Wang, J., Wang, Y., Zhang, Y., Uliana, A., Zhu, J., Liu, J. & Van der Bruggen, B. (2016). Zeolitic imidazolate framework/graphene oxide hybrid nanosheets functionalized thin film nanocomposite membrane for enhanced antimicrobial performance. *ACS Applied Materials & Interfaces*, *8*(38), 25508–25519. https://doi.org/10.1021/acsami.6b06992
43. Wang, X., Hou, J., Chen, F. & Meng, X. (2020). In-situ growth of metal-organic framework film on a polydopamine-modified flexible substrate for antibacterial and forward osmosis membranes. *Separation and Purification Technology*, *236*, 116239. https://doi.org/10.1016/j.seppur.2019.116239
44. Xie, H., Liu, X., Huang, Z., Xu, L., Bai, R., He, F., Wang, M., Han, L., Bao, Z., Wu, Y., Xie, C. & Gong, Y. (2022). Nanoscale zeolitic imidazolate framework (ZIF)–8 in cancer theranostics: Current challenges and prospects. *Cancers*, *14*(16), 3935. https://doi.org/10.3390/cancers14163935
45. Xiong, Y., Shu, Y., Deng, N., Luo, X., Liu, S. & Wu, X. (2024). A novel modified ZIF-8 nanoparticle with enhanced interfacial compatibility and pervaporation performance in a mixed matrix membrane for de-alcoholization in low-concentration solutions. *Molecules*, *29*(18), 4465. https://doi.org/10.3390/molecules29184465
46. Zhan, X., Gao, K., Jia, Y., Deng, W., Liu, N., Guo, X., Li, H. & Li, J. (2023). Enhanced desulfurization performance of ZIF−8/PEG MMMs: Effect of ZIF−8 particle size. *Membranes*, *13*(5), 515. https://doi.org/10.3390/membranes13050515
47. Zhang, M., Wang, X., Lin, R., Liu, Y., Chen, F., Cui, L., Meng, X. & Hou, J. (2021). Improving the hydrostability of ZIF-8 membrane by biomolecule towards enhanced nanofiltration performance for dye removal. *Journal of Membrane Science*, *618*, 118630. https://doi.org/10.1016/j.memsci.2020.118630
48. Zinah M. Mahdi, Manar A. Ehmud & Duaa S. Khazaal. (2022). Treatment of Wastewater using Bioflocculant Produced by Serratia marcesens and Pseudomonas aeruginosa. *Indian Journal of Environmental Protection*, *42*(9), 1141–1145.